IJMF, Iranian Journal of Materials Forming, Vol. 2, No. 1, pp 43-50
Printed in The Islamic Republic of Iran, 2015

Interaction between Precipitation and Dynamic Recrystallization in HSLA-100 Microalloyed Steel

G.R. Ebrahimi*[1], A. Momeni[2] and H. Eskandari[3]

[1]Department of Materials and Polymer Engineering, Hakim Sabzevari University, Sabzevar, Iran
[2]Department of Materials Science and Engineering, Hamedan University of Technology, Hamedan, Iran
[3]Department of Civil Engineering, Faculty of Engineering, Hakim Sabzevari University, Sabzevar, Iran

Abstract: Strain induced precipitation in HSLA-100 steel was investigated by conducting hot compression and relaxation tests at temperature range of 850°C to 1100°C and strain rate of 0.001 s^{-1} to $1s^{-1}$. The absence of dynamic recrystallization at temperatures below 1000°C was attributed to the influence of dynamic precipitation. The stress relaxation tests showed that strain induced precipitation is possible over a wide range of temperatures from 850°C to 1050°C. The starting and finishing times of precipitation were sensitive to temperature than strain rate. At temperature range of 950-1000°C and strain rate of $0.1s^{-1}$ the lowest times for precipitation were observed. The combination of precipitation-time-temperature and recrystallization-time temperature diagrams showed that at high temperatures and low strain rates, precipitation precedes dynamic recrystallization, whereas at the opposite condition, dynamic recrystallization goes in advance. The starting and finishing times for dynamic precipitation were approximated about 40 percent lower that those for strain induced precipitation.

Keywords: Hot deformation, Cu-bearing HSLA steel, Dynamic recrystallization, Hot compression, Stress relaxation

1. Introduction

Microalloyed (MA) high strength steels are widely used as alternatives for plain carbon and structural steels. They are used in automotive parts, line pipes and bridges [1]. The combination of high strength and low cost in these materials is due to the presence of a little amount (<0.1%) of microalloying elements such as Ti, Nb and V. Despite their attractiveness, the precise control of the processing route at high temperature deformation is required to obtain the optimized mechanical properties. Within MA steels, HSLA-100 is a relatively new alloy which takes the benefit of further hardening by the precipitation of copper-containing particles [2-5].

A comprehensive understanding of the hot deformation characteristics of this alloy is crucial to the proper design of its processing route. The different versions of controlled rolling such as conventional controlled rolling (CCR), recrystallization controlled rolling (RCR), and dynamic recrystallization controlled rolling (DRCR) have been developed according to the basic knowledge about the hot deformation behavior of different alloys [6-10].

The precipitation of microalloying carbonitrides is often promoted by the deformation at high temperatures and plays an important role in the microstructural and mechanical design of the MA steels. It

Received by the editors February 27, 2015; Revised March 19, 2015 and Accepted March 27, 2015.
*Corresponding author (ebrahimi@hsu.ac.ir)

has been well known that the strain induced precipitation (SIP) of carbides or carbonitrides in austenite can effectively pin the grain boundaries and inhibit their migration which is the early stage of recrystallization [11-15]. It is thought that fine precipitates have stronger influence on the static recrystallization (SRX) than the dynamic recrystallization (DRX) [16]. This is the concept of the RCR process in which the consecutive hardening and inter-pass static recrystallization are adopted to considerably refine austenite grain structure, thereby refining the resultant ferrite at low temperatures [17]. The influence of SIP on the hot deformation behavior of different steel grades has been studied and documented over years [18-20]. But for some newly developed steels such as HSLA-100, the conditions at which SIP occurs and its results on the softening processes during hot deformation need to be further studied. Indeed, it is very useful and applicable to develop a window, which clarifies the interaction between precipitation and recrystallization at different deformation conditions. The present investigation is devoted to address the hot deformation behavior of HSLA-100 steel with special attention to the interaction of strain induced precipitation and recrystallization. The potential of SIP and the interaction of precipitation with DRX are probed in the current research using hot compression and stress relaxation tests.

2. Experimental Procedures

The chemical composition of HSLA-100 microalloyed steel used in the present investigation is given in Table 1. The alloy was sand cast and then refined by electro slag remelting (ESR) process. Cylindrical specimens with 15 mm height and 10 mm diameter were machined for mechanical testing according to the ASTM E209 standard. The specimens were solutionized for 1 hour at 1200ºC and then cooled down to the deformation temperature. Graphite powder was applied on the contacting surfaces to reduce friction and minimize the samples barreling. The hot compression tests were performed at temperatures of 850ºC, 900ºC, 950ºC, 1000ºC, 1050ºC and 1100ºC and strain rates of $0.001s^{-1}$ following a 3 minutes soaking at the test temperature.

Table 1. Chemical composition of HSLA-100 microalloyed steel

Element	C	Mn	Si	P	S	Cu	Cr	Mo	Ni	Nb	Ti	V
Composition (wt %)	0.04	0.78	0.25	0.008	0.006	1.72	0.62	0.64	3.55	0.033	0.009	0.015

Strain relaxation (SR) tests were used to study strain induced precipitation. The details of the method have been described in the literature [21]. The SR tests were carried out by applying a pre-strain of 5% with different strain rates of $0.001s^{-1}$ to $1\ s^{-1}$ and temperatures of 850ºC to1050ºC (with the interval of 50 ºC). The pre-strain was adopted as low as 5% to avoid the occurrence of SRX during the relaxation of stress. The grain boundary movement during SRX eliminates the dislocation structure which affects the formation of carbonitride precipitates. After performing the prestrain, the variation of stress at the constant stain was recorded with time.

3. Results and Discussion

Figure 1 shows representative true stress-strain curves calculated from load-displacement data at various temperatures and strain rates. The influence of temperature seems to be more pronounced than that of strain rate. While at low temperatures, i.e. below 1000ºC, the flow curves are characterized by work hardening, at higher temperatures, flow curves are characterized by the peaks which are generally typical of DRX. One reason for this behavior can be the retarding affect of the dynamic precipitation of NbCN on DRX. The interaction between DRX and precipitation of microalloying carbonitrides has been studied by

mechanical testing elsewhere [22]. One of the mechanical testing methods to assess the possibility of precipitation during hot working is SR testing [21]. Figure 2 illustrates the results of the SR tests for different hot deformation conditions. The inflection points on the decreasing trend of stress versus logarithmic time in Fig. 2 can be attributed to the start and finish of SIP [21]. It is observed that the start and finish times of SIP (t_s and t_f) are more dependent on temperature than strain rate. The lowest t_s and t_f are observed at about 950ºC and they increase at low or high temperatures. The previous reports in the literature have shown that this temperature is corresponding to no recrystallization temperature (T_{nr}) of the alloy due to the precipitation of NbCN precipitates [22, 23]. Figure 3 shows the precipitation-time-temperature (PTT) diagram for SIP at constant strain rate of $0.1s^{-1}$. At the nose temperature, i.e. 950ºC, the shortest start and end times for SIP are about 10 and 1000 seconds, respectively. These times are important because they can be used to assess the interaction between DRX and precipitation. In addition, t_s and t_f for dynamic precipitation (DP) can be measured from those of SIP. It should be noted that SIP refers to a precipitation during stress relaxation tests where strain retains constant. But, DP refers to precipitation during straining, for example during hot compression. It has been experimentally known that DP is about an order of magnitude faster than SIP [16]. Since SIP occurs particularly rapidly at around 950ºC, therefore it is expected that the maximum interaction of DRX and DP may occur at the same temperature. Figures 4a and b indicate that t_s and t_f for SIP are minimized at $0.1s^{-1}$ and increased at higher or lower strain rates. It is also worthy of note that the nose temperature, which is also associated with T_{nr}, remains constant about 950-970ºC. Therefore, one can conclude that T_{nr} of the alloy is not significantly sensitive to strain rate.

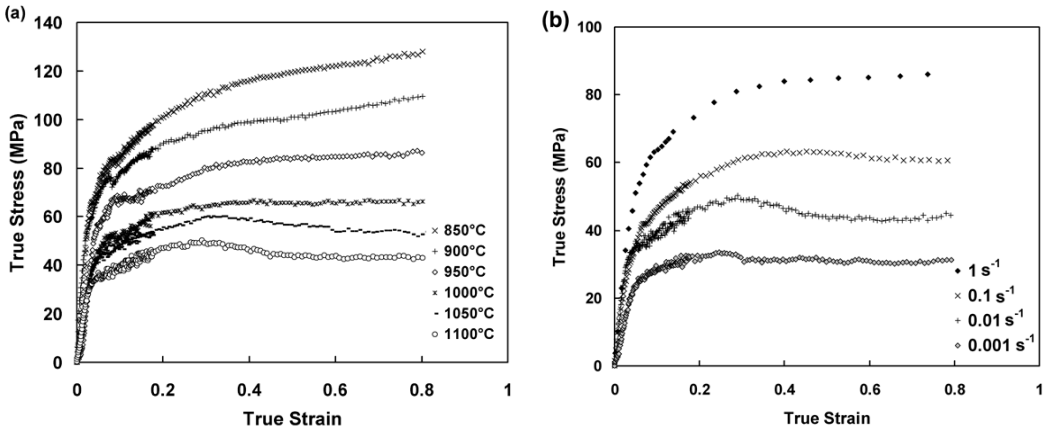

Fig. 1. Representative flow curves at (a) constant strain rate of $0.01s^{-1}$ and (b) constant temperature of 1100°C.

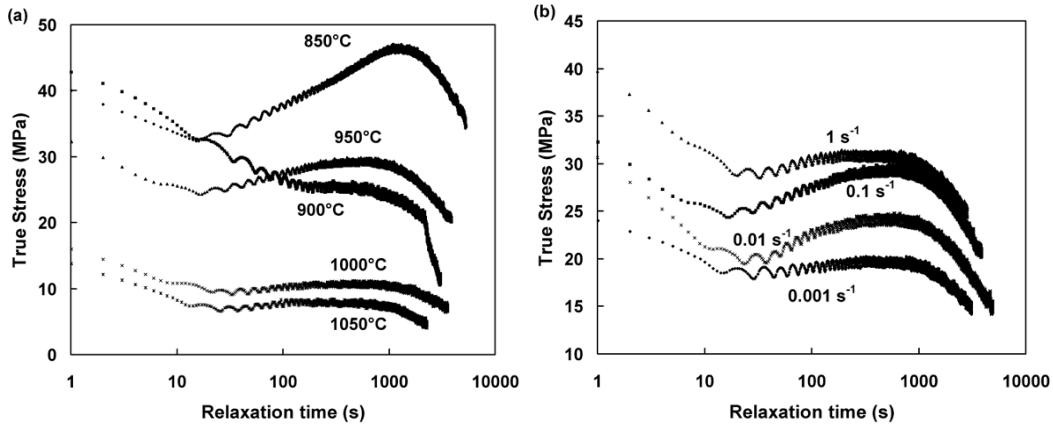

Fig. 2. Stress relaxation tests at (a) constant strain rate of $0.1s^{-1}$ and (b) constant temperature of 950°C.

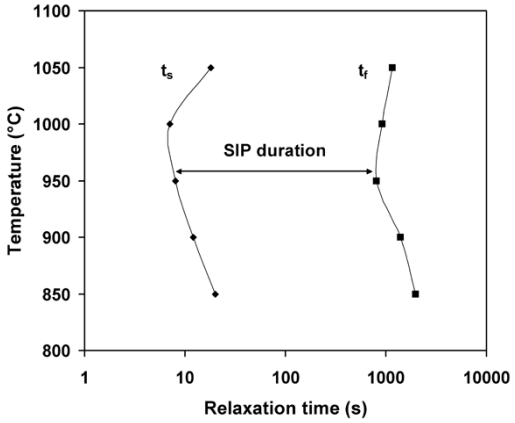

Fig. 3. Precipitation-time-temperature (PTT) curve obtained at constant strain rate of $0.1s^{-1}$.

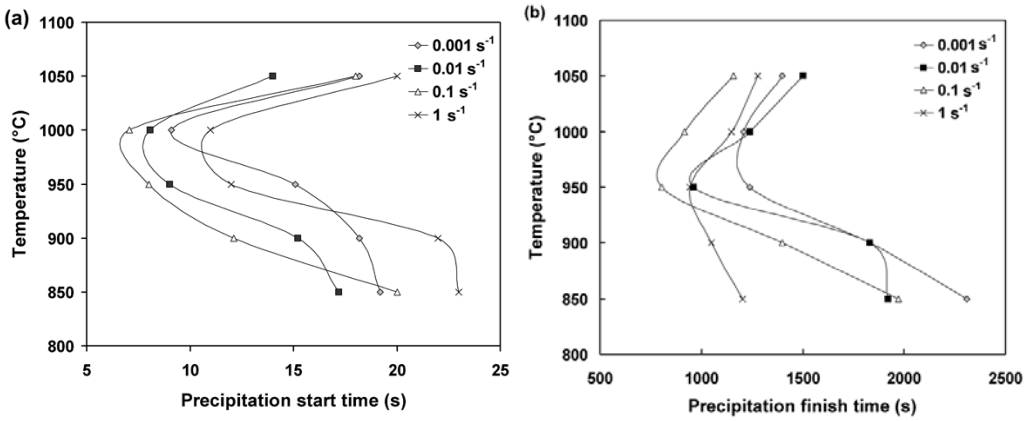

Fig. 4. Curves of (a) precipitation start (t_s) and (b) precipitation finish, (t_f) as a function of pre-strain rate.

In order to address the influence of strain rate on t_s and t_f and why $0.1s^{-1}$ is the critical rate, we should refer to the influence of pre-strain on the precipitation. Indeed, deformation favors the formation of fine carbonitrides, through SIP or DP, by two mechanisms; first, strain energy stimulates the formation of fine precipitates and second, dislocations formed facilitate diffusion. From this point of view, increasing strain rate augments both the stored strain energy and dislocation density and therefore leads to SIP or DP. On the other hand, increasing strain rate increases the potential of SRX or DRX in different ways. The moving high angle grain boundaries during SRX, even if partly, sweep away the dislocations and consequently postpone SIP. This situation is the case at strain rates higher than $0.1s^{-1}$.

The PTT curves are important for analyzing the potential of interaction between SIP and SRX during RCR processing or between DP and DRX during continuous single-hit hot deformation. Using this capability, the recrystallization-time-temperature (RTT) curves should be superimposed on the PTT curves. The RTT curves indicate the start and end times of recrystallization (DRX or SRX) as a function of temperature at a given strain rate. The starting time of DRX ($t_{s\,DRX}$) can be defined as follows:

$$t_{s\,DRX} = \frac{\varepsilon_p}{\dot{\varepsilon}} \tag{1}$$

Here, ε_p is the peak strain, which is directly obtained from the flow curve. Figure 5 shows the dependence of ε_p on deformation temperature at different strain rates. As expected, the peak strain decreases with increasing temperature and decreasing strain rate. This, in turn, indicates that high temperatures decrease

the time required for the initiation of DRX. The starting times of DRX ($t_{s\,DRX}$) are calculated from Eq. (1) using ε_p obtained from Fig. 5. Figure 6 shows the curves of $t_{s\,DRX}$ superimposed on the developed PTT curves at different strain rates. The results of Fig. 6 can be used to analyze the interaction of DP with DRX. It is observed that the curves of DP, are observed at shorter times respecting the SIP curves and therefore interact with $t_{s\,DRX}$ at different temperatures.

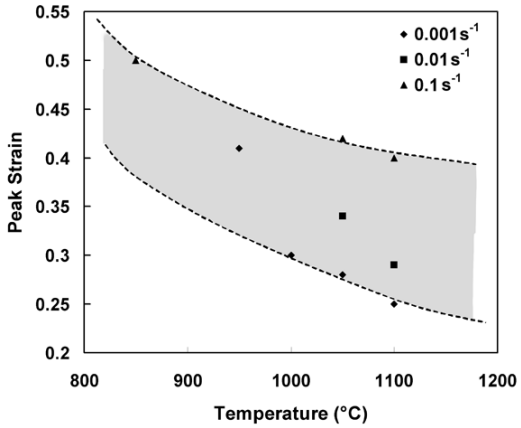

Fig. 5. Dependence of the peak strain for dynamic recrystallization on deformation temperature used for the determination of DRX start time ($t_{s\,DRX}$).

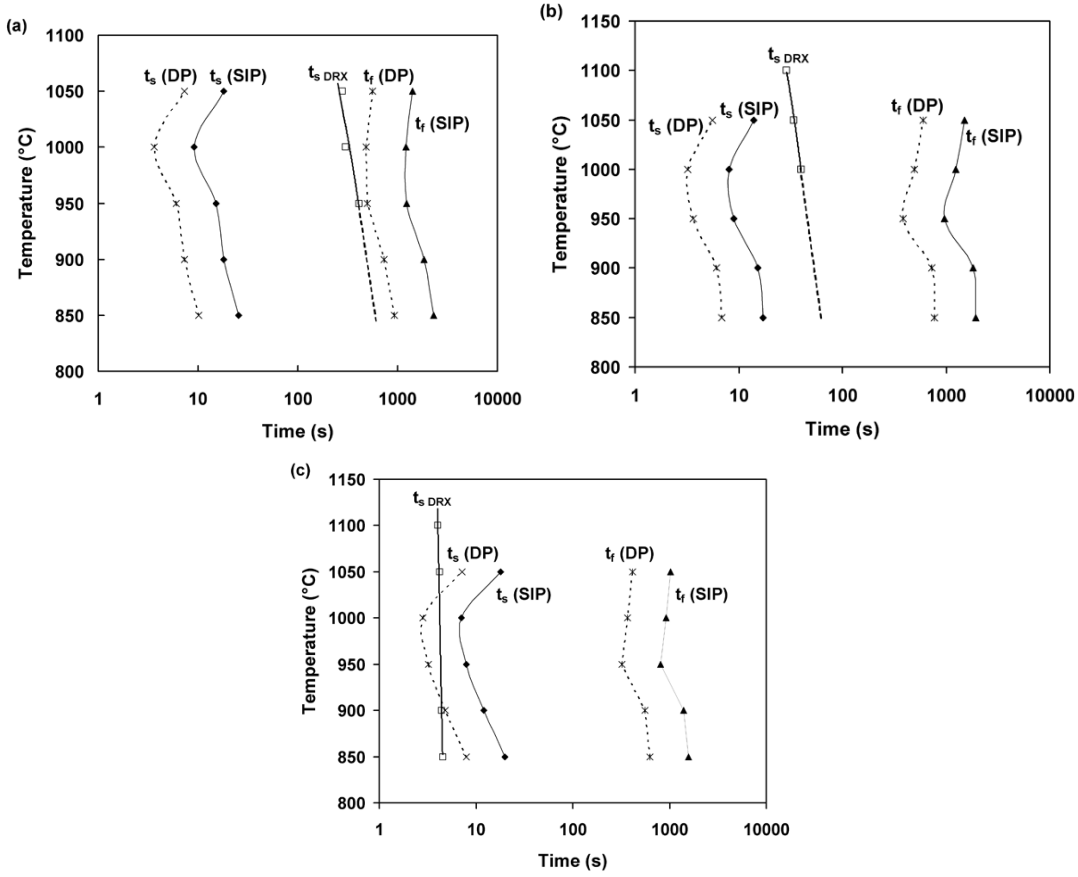

Fig. 6. Diagrams representing the combination of recrystallization-time-temperature (RTT) and precipitation-time-temperature (PTT) curves at pre-strain rates of (a) $0.001s^{-1}$, (b) $0.01s^{-1}$ and (c) $0.1s^{-1}$. SIP and DP respectively refers to strain induced precipitation and dynamic precipitation.

In agreement with Eq. (1), it is clearly seen that $t_{s\,DRX}$ increases as temperature declines. This is due to the fact that ε_p increases with decreasing temperature. At low strain rates of $0.001s^{-1}$ and $0.01\ s^{-1}$ (Figs. 6a and b), it is clearly seen that DP precedes DRX. In such cases, dynamic precipitation consumes the strain energy and therefore pushes the start of DRX to the longer times than expected. However, as strain rate rises to $0.1\ s^{-1}$, (Fig. 6c), $t_{s\,DRX}$ moves to shorter times and gets closer to the t_s (DP) and t_f (DP) curves. This indicates that, strain rate has stronger influence on the kinetics of DRX than temperature. At $0.1s^{-1}$ (Fig. 6c), the curves of $t_{s\,DRX}$ and t_s (DP) coincide at some temperatures. The missing data points of $t_{s\,DRX}$ at 950°C and 1000°C are attributed to the occurrence of DP before DRX. It is fair to say that at 950°C and 1000°C DP, it occurs fast and postpones DRX to higher strains beyond the strain of 0.8 adopted in the tests. On opposition, at higher or lower temperatures, DRX goes in advance to DP. Therefore, the curve of t_s (DP) should be drawn so that $t_{s\,DRX}$ at 950°C and 1000°C is located inside the DP region. Using this technique, t_s (DP) and t_f (DP) curves can be drawn based on the results of the flow curves shown in Fig. 1. It is observed that the calculated t_s (DP) and t_f (DP) are approximately 40% lower than t_s (SIP) and t_f (SIP), respectively. At high strain rates, i.e. beyond $0.1s^{-1}$, DRX commences earlier than DP, but increasing strain rate pushes the peak to high strains and makes it hardly discernible on the flow curves. Hence, the first step for analyzing the interaction between DRX and DP is to study the variation of ε_p with deformation temperature and strain rate. Figure7 illustrates the variation of peak strain and stress as a function of the Zener-Hollomon parameter. The value of apparent activation energy used to calculate Z has been taken as 377 kJ/mol determined in the previous paper [20]. The changes observed in the dependence of ε_p and σ_p on Z seems to be related to the interaction of DRX and DP. In agreement with the previous results, at high Z values, actually lnZ> 35, where DRX goes in advance to DP, as mentioned, the slope changes. In the same position, the behavior of σ_p is slightly changed. Therefore, lnZ=35 seems to be the boundary between two regions, pure DRX (lnZ>35) and DRX following DP (lnZ<35). Another boundary may be considered as lnZ=40 representing a condition beyond which DRX is shifted to very high strains so that it will be actually impossible in common industrial processes. The boundaries mentioned above can be represented in a frame of strain rate and temperature as a mechanism map in Fig. 8.

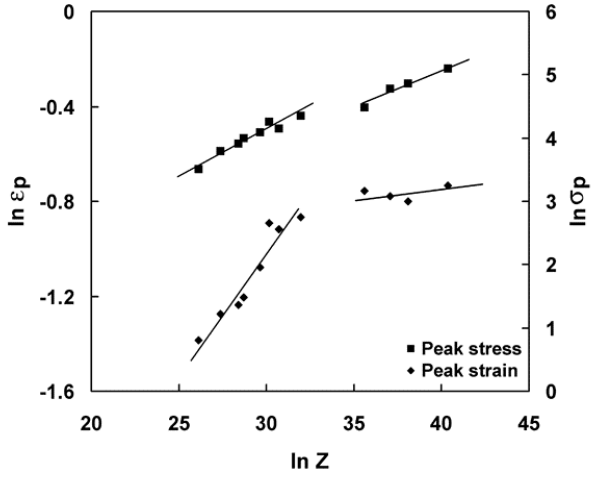

Fig. 7. Variation of peak strain and stress with the Z parameter, representing different microstructural mechanisms at low and high Z values.

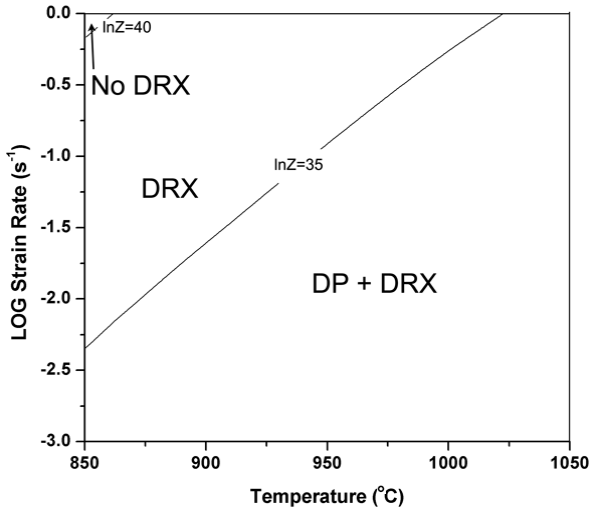

Fig. 8. Mechanism map illustrating the regions of different interaction of dynamic recrystallization and dynamic precipitation in the frame of strain rate and temperature.

4. Conclusion

Strain induced precipitation was investigated in HSLA-100 by hot compression testing. The noticeable results are listed below:

1- Stress relaxation tests showed that strain induced precipitation is possible over a wide range of temperature from 850°C to 1050°C.

2- The starting and ending times of precipitation were more sensitive to temperature than pre-strain rate.

3- At temperature range of 950-1000°C and pre-strain rate of $0.1s^{-1}$, the lowest starting and ending times of precipitation were observed.

4- The combination of precipitation-time-temperature and recrystallization-time temperature diagrams showed that at low Z values (lnZ<35) precipitation precedes dynamic recrystallization, whereas at higher Z, value dynamic recrystallization goes in advance.

5. References

[1] W. B. Marison, Overview of microalloying in steel, *Proceedings of the vanitec symposium on the use of vanadium in steel*, Giulin, China, 2000, 25-35.

[2] A. Ghosh, B. Mishra, S. Das and S. Chatterjee, Microstructure, properties, and age hardening behavior of a thermomechanically processed ultralow-carbon Cu-bearing high-strength steel, *Met. Mater. Trans*., 36A (2005) 703-713.

[3] Ghosh, Samar Das, S. Chatterjee, B. Mishra and P. Ramachandra Rao, Influence of thermo-mechanical processing and different post-cooling techniques on structure and properties of an ultra low carbon Cu bearing HSLA forging, *Mater. Sci. Eng*., A348 (2003) 299-308

[4] S. Panwar, D.B. Goel and O.P. Pandey, Effect of cold work and aging on mechanical properties of a copper bearing HSLA-100 steel, *Bull. Mater. Sci*., 28 (2005) 259-265.

[5] S. Panwar, D.B. Goel, O. P. Pandey and K. Prasad, Aging of a copper bearing HSLA-100 steel, *Bull. Mater. Sci*., 26 (2003) 441-447.

[6] M. Arribas, B. López and J.M. Rodriguez-Ibabe, Additional grain refinement in recrystallization controlled rolling of Ti-microalloyed steels processed by near-net-shape casting technology, *Mater. Sci. Eng*., A485 (2008) 383-394.

[7] M. Mirzaee, H. Keshmiri, G.R. Ebrahimi and A. Momeni, Dynamic recrystallization and precipitation in low carbon low alloy steel 26NiCrMoV 14-5, *Mater. Sci. Eng*., A551 (2012) 25– 31.

[8] P. Korczak, Influence of controlled rolling condition on microstructure and mechanical properties of low carbon micro-alloyed steels, *J. Mater. Process. Technol*., 157-158 (2004) 553-556.

[9] J.H. Bianchi and L.P. Karjalainen, Modelling of dynamic and metadynamic recrystallisation during bar rolling of a medium carbon spring steel, *J. Mater. Process. Technol*., 160 (2005) 267-277. .

[10] A. Momeni and S.M. Abbasi, On the opposition of dynamic recrystallization and solute dragging in steels, *J. Alloys Comp*. 622 (2015) 318–326.

[11] M. Gómez, L. Rancel, B.J. Fernández and S.F. Medina, Evolution of austenite static recrystallization and grain size during hot rolling of a V-microalloyed steel, *Mater. Sci. Eng*., A501 (2009) 188-196.

[12] J. Yang, Q. Liu, D. Sun and X. Li, Recrystallization behavior of deformed austenite in high strength microalloyed pipeline steel, *J. Iron and Steel Res. Int*., 16 (2009) 75-80.

[13] A. Momeni, S. Kazemi, G.R. Ebrahimi and A. Maldar, Dynamic recrystallization and precipitation in high manganese austenitic stainless steel during hot compression, *Int. J. Miner. Met. Mater*., 21 (2014) 36-44.

[14] O. Kwon and A.J. DeArdo, Interactions between recrystallization and precipitation in hot-deformed microalloyed steels, *Acta Metal. Mater*., 39 (1991) 529-538.

[15] G.R. Ebrahimi, A. Momeni, M. Jahazi and P. Bucher, Dynamic recrystallization and precipitation in 13Cr super-martensitic stainless steels, *Met. Mater. Trans*., 45A (2014) 2219-2231.

[16] J.J. Jonas, M.G. Akben and G.E. Ruddle, Mechanical testing for the study of austenite recrystallization and carbonitride precipitation, *Proceedings Japan-Canada seminar on secondary steel making*, 1985 234-246.

[17] T. Siwecki and G. Engberg, Recrystallization controlled rolling of steel, *Int. Conf. on Thermomechanical Processing in Theory, Modelling & Practice*, Stockholm, Sweden, 1997 121-143.

[18] A. Momeni, K. Dehghani, H. Keshmiri and G.R. Ebrahimi, Hot deformation behavior and microstructural evolution of a superaustenitic stainless steel, *Mater. Sci. Eng*., A 527 (2010) 1605–1611.

[19] H. Wu, L. Du and X. Liu, Dynamic recrystallization and precipitation behavior of Mn-Cu-V weathering steel, *J. Mater. Sci. Technol*., 27 (2011) 1131-1138.

[20] M. Mirzaee, H. Keshmiri, G.R. Ebrahimi and A. Momeni, Dynamic recrystallization and precipitation in low carbon low alloy steel 26NiCrMoV 14-5, *Mater. Sci. Eng*., A551 (2012) 25-31.

[21] W. J. Liu and J. J. Jonas, A stress relaxation method for following carbonitride precipitation in austenite at hot working temperatures, *Met. Mater. Trans*., 19A (1988) 1403-1413.

[22] A. Momeni, H. Arabi, A. Rezaei, H. Badri and S.M. Abbasi, Hot deformation behavior of austenite in HSLA-100 microalloyed steel, *Mater. Sci. Eng*., A 528 (2011) 2158–2163.

[23] N. Radovic, Correlation between apparent activation energy for hot working and temperature of no recrystallization in microalloyed steels, *Mater. Sci. Forum*, 426-432 (2003) 1553-1558.